Int. J. Heat Mass Transfer. Vol. 28, No. 1, pp. 17–23, 1985
Printed in Great Britain

0017–9310/85 $3.00 + 0.00

Analysis of two-dimensional radiative heat transfer in a gray medium with internal heat generation*

W. W. YUEN and C. F. HO
Department of Mechanical and Environmental Engineering, University of California, Santa Barbara, CA 93106, U.S.A.

(*Received* 20 *December* 1983 *and in revised form* 18 *April* 1984)

Abstract—Radiative heat transfer in a two-dimensional rectangular enclosure with gray medium and internal heat generation is considered. Solutions are generated by a point allocation technique in which unknown temperature profiles are expressed as polynomials. Based on a recently developed generalized exponential integral function, the present solution technique is demonstrated to be computationally more efficient than most of the conventional solution methods. For the case with constant internal heat generation, numerical solutions for temperature and heat flux distributions for enclosures of different optical thicknesses and aspect ratios are obtained. Analytical solutions are developed in the optically thin limit. Both the optical thickness and the enclosure geometry are demonstrated to have strong effects on the temperature distribution within the medium. The average heat transfer to the different boundaries, on the other hand, appears to depend mainly on the enclosure geometry.

1. INTRODUCTION

IN THE analysis of heat transfer in furnaces and other large-scale combustion systems, the importance of radiation is well known [1]. Indeed, a numerical technique which can deal effectively with the mathematical complexity of multi-dimensional radiative heat transfer in a heat generating system is indispensable for a quantitative analysis of furnace performance. In recent years, a large number of work has been reported and many solution techniques have been proposed in the general area of multi-dimensional radiative transfer [2–8]. Most of them, however, deal only with medium without internal heat generation. It is important to note that because of the integral-equation nature of the problem, the mathematical behavior of the governing equations for radiative transfer with internal heat generation and those without can be quite different. A solution technique or approximation procedure which is effective for the analysis of radiative transfer without internal heat generation can be relatively ineffective for problems with internal heat generation. The diffusion approximation, for example, has been very effective in generating accurate temperature distribution for a one-dimensional planar system at radiative equilibrium. It is relatively ineffective in generating accurate temperature distribution for the same planar system with internal heat generation. Currently, reported analysis on multi-dimensional radiative transfer with heat generation, either approximate or exact, are quite rare. Some limited results on a rectangular enclosure generated by Modest [4] and Howell and co-workers [5, 6] appear to be the only reported numerical data available in the literature. They are quite insufficient either to demonstrate the effectiveness of their solution technique for this class of problems or to illustrate the general heat transfer behavior of a multi-dimensional radiating heat-generating system.

In a recent publication [9], the point allocation method, together with the introduction of a generalized exponential integral function, was demonstrated to be effective in the analysis of two-dimensional radiative equilibrium. Detailed temperature and heat flux distributions were generated with relatively little computational complexity. The objective of the present work is to demonstrate that the technique can be equally effective for problems with internal heat generation. Expressed in terms of the generalized exponential integral function, the governing equations are shown to be solvable analytically both in the optically thick and thin limits. Exact limiting expressions for temperature and heat flux distributions are obtained. As in the case without heat generation, evaluations of only single integrals are required for numerical solutions. Compared to the standard Hottel zonal method which requires evaluation of double integrals, the present technique is thus more efficient computationally. For a two-dimensional rectangular enclosure with constant internal heat generation, heat flux and temperature distributions for different optical thickness and aspect ratio are generated based on the present technique. Some interesting conclusions on the general heat transfer characteristics of a multi-dimensional radiating heat-generating system are deduced.

2. MATHEMATICAL FORMULATION

The physical model and its associated coordinate system is shown in Fig. 1. For simplicity, the four boundaries are assumed to be black isothermal surface with zero emissive power. It can be readily shown that

* This work is based upon work supported by the National Science Foundation Grant No. MEA 80-24824.

NOMENCLATURE

a	absorption coefficient
$d(\eta,\eta',\zeta,\zeta')$	function defined by equation (7)
$G_\eta(\eta,\zeta)$	dimensionless heat flux defined by equations (3) and (5)
$G_\zeta(\eta,\zeta)$	dimensionless heat flux defined by equations (3) and (6)
$H(\eta,\zeta)$	internal heat generation rate
H_0	characteristic heat generation rate
$h(\eta,\zeta)$	dimensionless internal heat generation rate defined by equation (3)
L_1	optical thickness of the enclosure in the y-direction
L_2	optical thickness of the enclosure in the z-direction
M_{ij}	function in equation (26)
NY_{ij}	function in equation (27)
P_{ij}	coefficients of assumed polynomial defined by equation (25)
$\mathbf{Q}$	heat flux vector
r	'polar' coordinate utilized by equations (9)–(11)
$\mathbf{r}$	position vector
$S_n(x)$	exponential integral function
T	temperature
y	coordinate
Y	half-width of the rectangular enclosure
z	coordinate
Z	half-height of the rectangular enclosure.

Greek symbols

ζ	optical thickness variable in the z-direction
η	optical thickness variable in the y-direction
θ	blackbody emissive power
θ_g	dimensionless emissive power
ϕ	angular coordinate utilized by equations (9)–(11)
σ	Stefan–Boltzman constant.

based on superposition, solutions to a rectangular enclosure problem with arbitrary constant surface temperature and internal heat generation can be generated from the present result and those presented in the previous work [9]. From standard reference [10], the energy equation for the medium is given by

$$4\theta(\mathbf{r}) = \int_V \theta(\mathbf{r}')\frac{e^{-a|\mathbf{r}-\mathbf{r}'|}}{\pi|\mathbf{r}-\mathbf{r}'|^2}\,a\,dV(\mathbf{r}') + \frac{H(\mathbf{r})}{a} \qquad (1)$$

where $\theta(\mathbf{r}) = \sigma T^4(\mathbf{r})$ is the blackbody emissive power, $\mathbf{r}'$ a point located at the interior of the medium $H(\mathbf{r})$ the internal heat generation rate and a the absorption coefficient which for the present work is assumed to be constant. Based on the medium's temperature which is determined by solution to equation (1), the radiative heat flux can be written as

$$\mathbf{Q}(\mathbf{r}) = \int_V \theta(\mathbf{r}')\frac{e^{-a|\mathbf{r}-\mathbf{r}'|}}{\pi|\mathbf{r}-\mathbf{r}'|^3}\,a(\mathbf{r}-\mathbf{r}')\,dV. \qquad (2)$$

As shown in the previous work [9], all integrals in the x-direction can be expressed in terms of the generalized exponential integral function $S_n(x)$. In terms of the following dimensionless variables

$$\eta = \frac{y}{Y}, \quad \zeta = \frac{z}{Z},$$

$$\theta_g(\eta,\zeta) = \frac{a\theta(\eta,\zeta)}{H_0}, \quad G(\eta,\zeta) = \frac{a\mathbf{Q}(\eta,\zeta)}{H_0},$$

$$h(\eta,\zeta) = \frac{H(\eta,\zeta)}{H_0}, \qquad (3)$$

$$L_1 = 2aY, \quad L_2 = 2aZ$$

with H_0 being a characteristic heat generation rate, equations (1) and (2) can be simplified to yield

$$\theta_g(\eta,\zeta) = \frac{L_1L_2}{16}\int_{-1}^{1}\int_{-1}^{1}\theta_g(\eta',\zeta')\times\frac{S_1(d)}{d}\,d\eta'\,d\zeta' + \frac{h(\eta,\zeta)}{4} \qquad (4)$$

$$G_\eta(\eta,\zeta) = \frac{L_1^2L_2}{8}\int_{-1}^{1}\int_{-1}^{1}\theta_g(\eta',\zeta')\frac{S_2(d)(\eta-\eta')}{d^2}\,d\eta'\,d\zeta' \qquad (5)$$

$$G_\zeta(\eta,\zeta) = \frac{L_1L_2^2}{8}\int_{-1}^{1}\int_{-1}^{1}\theta_g(\eta',\zeta')\frac{S_2(d)(\zeta-\zeta')}{d^2}\,d\eta'\,d\zeta' \qquad (6)$$

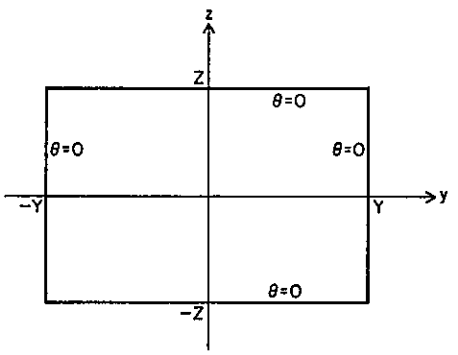

FIG. 1. Geometry and coordinate system for the two-dimensional rectangular enclosure problem.

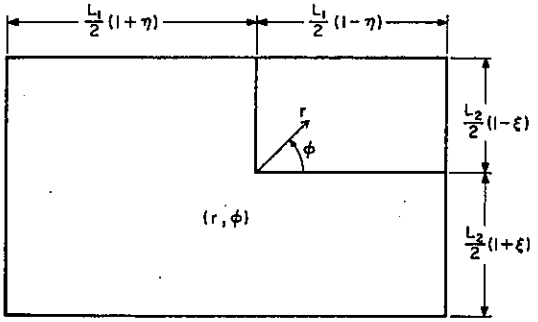

FIG. 2. Coordinate and domain of integration used in equations (9)–(11).

where

$$d(\eta,\eta',\zeta,\zeta') = \tfrac{1}{2}[L_1^2(\eta-\eta')^2 + L_2^2(\zeta-\zeta')^2]^{1/2} \quad (7)$$

and

$$S_n(x) = \frac{2}{\pi}\int_1^\infty \frac{e^{-xt}\,dt}{t^n(t^2-1)^{1/2}}. \quad (8)$$

Similar to the previous work [9], equations (4)–(6) are rewritten in terms of a polar coordinate (r,ϕ) to simplify the numerical computation. The relation between these coordinates and (η,ζ) is illustrated in Fig. 2. These equations become

$$4\theta_g(\eta,\zeta) = \int\int_{(r,\phi)} \theta_g\left(\eta+\frac{2r}{L_1}\cos\phi,\zeta + \frac{2r}{L_2}\sin\phi\right)S_1(r)\,dr\,d\phi + h(\eta,\zeta) \quad (9)$$

$$G_\eta(\eta,\zeta) = -\int\int_{(r,\phi)} \theta_g\left(\eta+\frac{2r}{L_1}\cos\phi,\zeta + \frac{2r}{L_2}\sin\phi\right)S_2(r)\cos\phi\,dr\,d\phi \quad (10)$$

$$G_\zeta(\eta,\zeta) = -\int\int_{(r,\phi)} \theta_g\left(\eta+\frac{2r}{L_1}\cos\phi,\zeta + \frac{2r}{L_2}\sin\phi\right)S_2(r)\sin\phi\,dr\,d\phi. \quad (11)$$

Equations (9)–(11) are the basic dimensionless governing equations for the present problem.

3. METHOD OF SOLUTION

3.1 *Limiting solutions*

In the optically thin limit, it can be readily observed that since the coordinate r has unit of optical thickness, the integral on the RHS of equation (9) approaches zero. The dimensionless emissive power and heat fluxes become

$$\theta_g(\eta,\zeta) = \frac{h(\eta,\zeta)}{4} \quad (12)$$

$$G_\eta(\eta,\zeta) = -\frac{S_2(0)}{4}\int\int_{(r,\phi)} h\left(\eta+\frac{2r}{L_1}\cos\phi,\zeta + \frac{2r}{L_2}\sin\phi\right)\cos\phi\,dr\,d\phi \quad (13)$$

and

$$G_\zeta(\eta,\zeta) = -\frac{S_2(0)}{4}\int\int_{(r,\phi)} h\left(\eta+\frac{2r}{L_1}\cos\phi,\zeta + \frac{2r}{L_2}\sin\phi\right)\sin\phi\,dr\,d\phi. \quad (14)$$

It is interesting to note that equations (12)–(14) suggest that for internal heat generation rates which can be expressed in simple analytical form (such as a power series), the temperature distribution is also analytic and the heat fluxes can be expressed analytically in terms of some shape-factor-like integrations. These interesting results will be presented in more detail in another publication [11]. For the present work, a constant internal heat generation $H(\eta,\zeta) = H_0$ is considered. Equations (12)–(14) become

$$\theta_g(\eta,\zeta) = \tfrac{1}{4} \quad (15)$$

$$G_\eta(\eta,\zeta) = \frac{1}{2\pi}\left[\eta_+\left(\tan^{-1}\frac{\zeta_+}{\eta_+} + \tan^{-1}\frac{\zeta_-}{\eta_+}\right) - \eta_-\left(\tan^{-1}\frac{\zeta_+}{\eta_-} + \tan^{-1}\frac{\zeta_-}{\eta_-}\right) + \frac{\zeta_+}{2}\log\left(\frac{\zeta_+^2+\eta_+^2}{\zeta_+^2+\eta_-^2}\right) + \frac{\zeta_-}{2}\log\left(\frac{\zeta_-^2+\eta_+^2}{\zeta_-^2+\eta_-^2}\right)\right] \quad (16)$$

and

$$G_\zeta(L_1,L_2,\eta,\zeta) = G_\eta(L_2,L_1,\zeta,\eta) \quad (17)$$

where

$$\eta_+ = \frac{L_1}{2}(1+\eta), \quad \eta_- = \frac{L_1}{2}(1-\eta) \quad (18)$$

$$\zeta_+ = \frac{L_2}{2}(1+\zeta), \quad \zeta_- = \frac{L_2}{2}(1-\zeta). \quad (19)$$

In the optically thick limit, a Taylor series expansion of $\theta_g(\eta,\zeta)$ in L_1^{-1} reduces equations (9)–(11) into the following familiar diffusion-like expressions

$$\frac{1}{L_1^2}\frac{\partial^2\theta_g}{\partial\eta^2} + \frac{1}{L_2^2}\frac{\partial^2\theta_g}{\partial\zeta^2} = -\frac{3}{16} \quad (20)$$

$$G_\eta = -\frac{8}{3L_1}\frac{\partial\theta_g}{\partial\eta}, \quad G_\zeta = -\frac{8}{3L_2}\frac{\partial\theta_g}{\partial\zeta}. \quad (21)$$

Solutions to equation (20) are well known from standard references [12].

Taking the limit of $L_1 \to \infty$ and utilizing the

following identity

$$E_n(x) = \frac{1}{2}\int_{-\pi/2}^{\pi/2} S_n(x\sec\phi)\cos^{n-2}\phi\, d\phi \quad (22)$$

equations (4) and (6) are reduced to

$$\theta_g(\zeta) = \frac{L_2}{4}\int_{-1}^{1}\theta_g\zeta' E_1\left[\frac{L_2}{2}\zeta-\zeta'\right]d\zeta' + \frac{1}{4} \quad (23)$$

$$G_\zeta(\zeta) = \frac{L_2}{2}\int_{-1}^{1}\theta_g\zeta' E_2\left[\frac{L_2}{2}\zeta-\zeta'\right]d\zeta'. \quad (24)$$

3.2 *Numerical solutions*

Similar to the previous work, the point allocation method is used to generate numerical solutions. Specifically, for the case with constant internal heat generation, the unknown temperature distribution is assumed to be a polynomial as follows:

$$\theta_g(\eta,\zeta) = \sum_{i=0}^{i=n}\sum_{j=0}^{j=n} P_{2i,2j}\eta^{2i}\zeta^{2j}. \quad (25)$$

Substituting equation (25) into equations (9) and (10), the following equations result

$$\sum_{i=0}^{i=n}\sum_{j=0}^{j=n} P_{2i,2j}[4\eta^{2i}\zeta^{2j} - M_{2i,2j}(\eta,\zeta,L_1,L_2)] = 1 \quad (26)$$

$$G_\eta(\eta,\zeta) = -\sum_{i=0}^{i=n}\sum_{j=0}^{j=n} P_{2i,2j}NY_{2i,2j}(\eta,\zeta,L_1,L_2). \quad (27)$$

The detailed expressions of $M_{2i,2j}(\eta,\zeta,L_1,L_2)$ and $NY_{2i,2j}(\eta,\zeta,L_1,L_2)$ are given in the previous work [9]. As demonstrated in the same work, only the numerical tabulation of a finite number of single integrals are required for the evaluation of these expressions. For any assumed polynomial expression, the temperature and heat flux distributions can thus be readily evaluated based on equations (26) and (27).

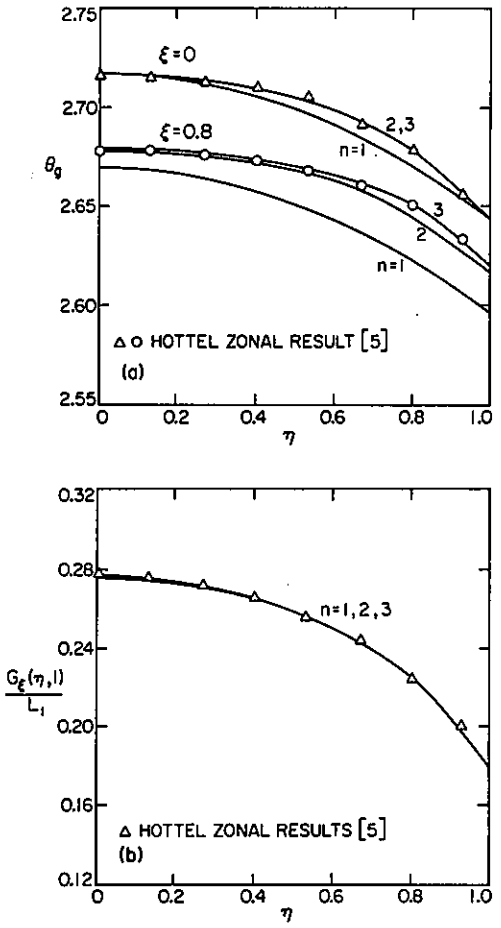

FIG. 3. (a) Comparison between the first three-order ($n = 1, 2, 3$) prediction of the medium temperature with the available Hottel zonal result ($L_1 = L_2 = 0.1$). (b) Comparison between the first three-order ($n = 1, 2, 3$) prediction of the heat flux at the top wall ($\xi = 1.0$) with available Hottel zonal result ($L_1 = L_2 = 0.1$).

4. RESULTS AND DISCUSSION

In the nth approximation, equation (26) is evaluated at $(n+1)^2$ locations $(\eta = i/n, \zeta = j/n, i,j = 0,n)$ to generate a set of algebraic equations for the unknown coefficients $P_{2i,2j}$. Since the functions $M_{2i,2j}(\eta,\zeta,L_1,L_2)$ and $NY_{2i,2j}(\eta,\zeta,L_1,L_2)$ can be readily evaluated, solutions are generated with little effort. Some typical temperature and heat flux distribution for $L_1 = L_2 = 0.1$ and $L_1 = L_2 = 1.0$, together with the corresponding results generated with a Hottel zonal method by Howell *et al.* [5, 6], are presented in Figs 3a,b, 4a,b. It can be readily observed that the third-order results are practically indistinguishable from those generated by the Hottel method. Indeed, the two results agree to within the second decimal figure for all cases. The same rapid rate of convergence is observed for all optical thickness ($L_1, L_2 = 0.1$, 0.5, 1.0, 2.0 and 5.0) considered in this work.

It is important to note that the selection of allocation points is not critical for the accuracy of the present approach. Accuracy can generally be assured if the selected points are distributed uniformly across the enclosure. In all cases, energy conservation (i.e. sum of heat transfer to the four boundaries = total energy generated within the enclosure) is achieved to within 0.1% by the third-order results.

Typical heat flux and temperature distributions for different values of L_1 and L_2 generated from third-order solutions are presented in Tables 1–3. More detailed distributions and solutions of the coefficient $P_{2i,2j}$ are summarized elsewhere [13].

Qualitatively, results presented in Tables 1–3 agree well with those expected from physical consideration. Both the enclosure's geometry and optical thickness have significant influences on the medium's temperature distribution. It is interesting to note, however, the heat flux distribution at the wall for a given enclosure geometry (L_1/L_2) appears to be quite insensitive to the optical thickness L_1. The optically thick and thin limit of the heat flux at the midpoint of a boundary,

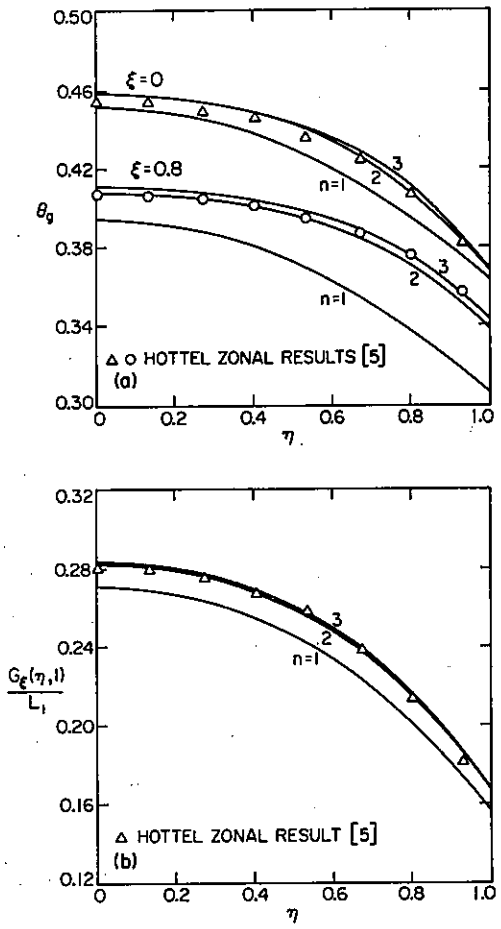

FIG. 4. (a) Comparison between the first three-order ($n = 1, 2, 3$) prediction of the medium temperature with the available Hottel zonal result ($L_1 = L_2 = 1.0$). (b) Comparison between the first three-order ($n = 1, 2, 3$) prediction of the heat flux at the top wall ($\xi = 1.0$) with the available Hottel zonal result ($L_1 = L_2 = 1.0$).

Table 1. Third-order result of the heat transfer at the top wall, $G_\xi(\eta, 1)/L_1$

L_1	L_2	$\eta = 0$	0.3333	0.6667	1.000
0.1	0.1	0.277	0.269	0.244	0.180
	0.5	0.489	0.480	0.448	0.327
	1.0	0.543	0.534	0.502	0.336
	2.0	0.565	0.556	0.525	0.304
	5.0	0.565	0.556	0.525	0.236
1.0	0.1	0.048	0.048	0.045	0.032
	0.5	0.191	0.185	0.163	0.112
	1.0	0.283	0.273	0.238	0.166
	2.0	0.353	0.341	0.301	0.206
	5.0	0.374	0.361	0.320	0.192
5.0	0.1	0.010	0.010	0.010	0.007
	0.5	0.050	0.049	0.047	0.031
	1.0	0.097	0.095	0.086	0.054
	2.0	0.177	0.170	0.144	0.088
	5.0	0.298	0.282	0.227	0.132

Table 2. Third-order result for the horizontal center-line temperature $\theta_g(\eta, 0)$

L_1	L_2	$\eta = 0$	0.4	0.6	1.0
0.1	0.1	0.272	0.271	0.270	0.264
	0.5	0.290	0.289	0.287	0.280
	1.0	0.296	0.295	0.293	0.286
	2.0	0.300	0.298	0.297	0.289
	5.0	0.301	0.300	0.299	0.291
1.0	0.1	0.296	0.295	0.293	0.274
	0.5	0.408	0.401	0.391	0.333
	1.0	0.500	0.487	0.469	0.385
	2.0	0.600	0.582	0.557	0.448
	5.0	0.686	0.663	0.633	0.505
5.0	0.1	0.301	0.301	0.301	0.274
	0.5	0.467	0.464	0.457	0.341
	1.0	0.686	0.672	0.648	0.415
	2.0	1.163	1.111	1.031	0.560
	5.0	2.466	2.270	2.009	0.923

$G_\eta(1, 0)/L_1$ are plotted as functions of the aspect ratio $R = L_1/L_2$ in Fig. 5. The remarkable similarity between the two curves suggests that either one of the two limiting solutions would be an adequate approximation of the actual heat transfer. Inspection of numerical results presented in Table 1 yields essentially the same conclusion. Indeed, general solutions to equations (13) and (14), which will be presented elsewhere [11], might be a sufficient first-order analytical approximation of the boundary heat flux distribution in a general two-dimensional heat generating radiating system.

In the development of approximation method in this area, many investigators demonstrate the effectiveness of the technique by the accuracy of its prediction of heat flux distribution at the boundary. The present result suggests that such criterion can be quite misleading. Since the heat flux distribution is relatively insensitive to optical thickness, it is not surprising that most of the existing approximation methods such as the differential

Table 3. Third-order result for the wall temperature $\theta_g(\eta, 1)$

L_1	L_2	$\eta = 0$	0.3333	0.6667	1.000
0.1	0.1	0.264	0.264	0.263	0.260
	0.5	0.272	0.271	0.271	0.267
	1.0	0.274	0,273	0.272	0.268
	2.0	0.274	0.274	0.273	0.269
	5.0	0.274	0.274	0.273	0.269
1.0	0.1	0.286	0.285	0.283	0.268
	0.5	0.350	0.345	0.339	0.302
	1.0	0.385	0.379	0.370	0.320
	2.0	0.409	0.402	0.392	0.338
	5.0	0.415	0.408	0.398	0.344
5.0	0.1	0.291	0.291	0.291	0.269
	0.5	0.397	0.395	0.389	0.309
	1.0	0.505	0.496	0.480	0.344
	2.0	0.676	0.651	0.613	0.389
	5.0	0.923	0.869	0.797	0.412

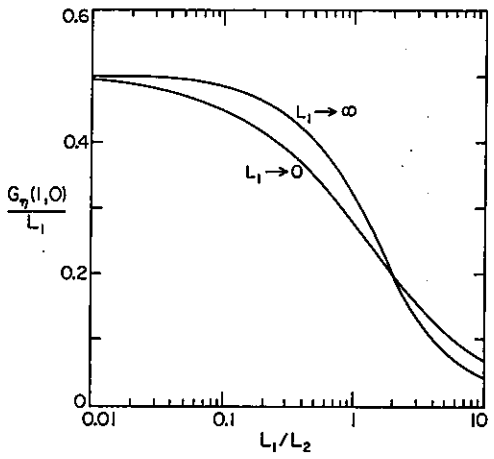

FIG. 5. Comparison between the optically thin and thin prediction of $G_\eta(1,0)/L_1$.

approximation [3, 4] and P–N method [5] yield accurate heat flux predictions. The applicability of these methods for practical system, however, would not be established until they demonstrate a capability of predicting the interior temperature distribution.

REFERENCES

1. J. De Ris, Fire radiation—a review, *The 17th Symposium (International) on Combustion*, p. 1003. The Combustion Institute (1979).
2. P. Cheng, Two-dimensional radiative gas flow by a moment method, *AIAA J.* **2**, 1662 (1964).
3. L. Glatt and D. B. Olfe, Radiative equilibrium of a gray medium in a rectangular enclosure, *J. Quant. Spectrosc. Radiat. Trans.* **13**, 881 (1973).
4. M. F. Modest, Radiative equilibrium of a gray medium in a rectangular enclosure bounded by gray walls, *J. Quant. Spectrosc. Radiat. Trans.* **15**, 445 (1975).
5. A. C. Ratzel and J. R. Howell, Two-dimensional radiation in absorbing–emitting–scattering media using the P–N approximation, ASME Paper 82-HT-19 (1982).
6. M. M. Razzaque, D. E. Klein, and J. R. Howell, Finite element solution of radiative heat transfer in a two-dimensional rectangular enclosure with gray participating media, ASME Paper 82-WA/HT-61 (1982).
7. W. F. Breig and A. L. Crosbie, Two-dimensional radiative equilibrium: a semi-infinite medium subjected to cosing varying radiation, *J. Quant. Spectrosc. Radiat. Trans.* **13**, 1395 (1973).
8. A. L. Crosbie and T. L. Linsenbardt, Two-dimensional isotropic scattering in a semi-infinite medium, *J. Quant. Spectrosc. Radiat. Trans.* **19**, 257 (1978).
9. W. W. Yuen and L. W. Wong, Analysis of radiative equilibrium in a rectangular enclosure with gray medium, *J. Heat Transfer* **106**, 433 (1984).
10. R. Siegel and J. R. Howell, *Thermal Radiation Heat Transfer*. McGraw-Hill, New York (1972).
11. W. W. Yuen and F. Chen, Analysis of radiative heat transfer in enclosures with a non-participating medium and internal heat generation: a physical interpretation of the geometric mean beam length, submitted for publication in *J. Heat Transfer*.
12. H. S. Carslaw and J. C. Jaeger, *Conduction of Heat in Solids*, 2nd ed. Oxford University Press, London, 1959.
13. W. W. Yuen, Numerical results of radiative heat transfer in a rectangular enclosure with gray medium at constant internal heat generation, UCSB Report No. ME-83-2 1983.

ANALYSE DU TRANSFERT RADIATIF BIDIMENSIONNEL DANS UN MILIEU GRIS AVEC GENERATION INTERNE DE CHALEUR

Résumé—On considère le transfert radiatif bidimensionnel dans une enceinte rectangulaire avec un milieu gris et une génération interne de chaleur. Des solutions sont obtenues par une technique d'allocation ponctuelle dans laquelle les profils de température inconnus sont exprimés de façon polynomiale. A partir d'une fonction intégrale exponentielle généralisée, la technique de résolution présente est montrée être numériquement plus efficiente que la plupart des méthodes conventionnelles. Dans le cas d'une génération interne de chaleur constante, on obtient des solutions numériques pour les températures et les flux de thermiques dans des enceintes d'épaisseur optique et de rapport de forme variés. Des solutions analytiques sont développées pour la limite optiquement mince. L'épaisseur optique et la géométrie de l'enceinte ont ensemble des effets importants sur la distribution de température dans le milieu. Le transfert thermique moyen aux frontières différentes, par contre, dépend principalement de la géométrie de l'enceinte.

ANALYSE DES ZWEIDIMENSIONALEN WÄRMEAUSTAUSCHES DURCH STRAHLUNG IN EINEM GRAUEN MEDIUM MIT INNEREN WÄRMEQUELLEN

Zusammenfassung—Der Strahlungswärmeaustausch in einem zweidimensionalen rechteckigen Gebiet, das ein graues Medium mit Wärmequellen enthält, wird untersucht. Die Lösungen werden mit Hilfe einer Punkteverteilungstechnik gewonnen, wobei unbekannte Temperaturprofile durch Polynome ausgedrückt werden. Ausgehend von einer kürzlich entwickelten allgemeinen Exponential-Integralfunktion wird gezeigt, daß die hier behandelte Lösungsmethode für Rechenmaschinen günstiger ist als die gebräuchlichen Lösungsmethoden. Bei konstanten inneren Wärmequellen ergeben sich numerische Lösungen für die Temperatur- und Wärmestromdichte-Verteilung in Hohlräumen mit verschiedenen optischen Dicken und Seitenverhältnissen. Für optisch dünne Schichten werden analytische Lösungen entwickelt. Es wird gezeigt, daß sowohl die optische Dicke wie auch die Hohlraum-Geometrie einen großen Einfluß auf die Temperaturverteilung innerhalb des Mediums haben. Dagegen hängt der mittlere Wärmetransport zu den verschiedenen Begrenzungen hin hauptsächlich von der Hohlraum-Geometrie ab.

АНАЛИЗ ДВУМЕРНОГО ЛУЧИСТОГО ТЕПЛОПЕРЕНОСА В СЕРОЙ СРЕДЕ С ВНУТРЕННИМ ИСТОЧНИКОМ ТЕПЛА

Аннотация—Рассмотрен лучистый теплоперенос в двумерной прямоугольной полости с серой средой и внутренним источником тепла. Задача решается методом нанесения точек, в котором искомые профили температуры можно представить многочленами. С помощью недавно предложенной обобщенной экспоненциальной интегральной функции показано, что такой метод решения в расчетном отношении более эффективен, чем большинство из применяемых методов решения. Для случая с постоянным внутренним источником тепла численно решена задача о распределении температур и теплового потока в полостях с различными значениями оптической толщины и отношения сторон. Получены аналитические решения в оптически тонком пределе. Показано, что как оптическая толщина, так и геометрия полости оказывают существенное влияние на распределение температур в среде. С другой стороны, величина усредненного теплового потока в разных направлениях, по-видимому, зависит в основном от геометрии полости.